

# Effect of Sr<sup>+</sup> ion Concentration on Microstructure and Dielectric properties of Barium Strontium Titanate Ceramics

Hamed A. Gatea<sup>1,\*</sup>, Hashim Abbas<sup>2</sup> and Iqbal S. Naaji<sup>3</sup>

<sup>1</sup>Department of Radiology, College of Health and Medical Technolgy, Al-Ayen University, Thi-Qar, Iraq

<sup>2</sup>Optermery Department, College of Health and Medical Technolgy, Al-Ayen University, Thi-Qar, Iraq

<sup>3</sup>Physics Department, College of Science, Baghdad university, Baghdad, Iraq

Received: 22 Feb. 2022, Revised: 2 Apr. 2022, Accepted: 12 Apr. 2022

Published online: 1 May 2022

**Abstract:** Ba<sub>1-x</sub>Sr<sub>x</sub>TiO<sub>3</sub>(BST) solid solution with x=0.3,0.4 and 0.5 were prepared by sol-gel method. (Ba, Sr) acetate and Titanate isopropoxide were used as a starting material. XRD patterns confirmed the formation of tetragonal perovskite structure and cubic structure. The FESEM images showed that the particles size reduced when strontium concentration increased. Particles size influence on dielectric constant which observed that with decreasing value dielectric constant due to increased frequency and strontium ion Sr<sup>+</sup>. The high value of dielectric constant observed at low frequencies and reduced concentration of Sr<sup>+</sup>.

**Keywords:** CeO<sub>2</sub> nanoparticles, PL spectra, Heat treatment, optical properties.

## 1 Introduction

Ferroelectric materials ubiquitous and mature materials for advanced technology. These ceramic materials are active elements in a range of piezoelectric, pyroelectric and ferroelectric devices [1]. It has been widely intensively investigated ferroelectrics and widely studied not only because of its variety of outstanding physical properties but also for its practical application [2]. It performs functions such as electronic applications in multilayer and voltage-tunable capacitors, nonvolatile ferroelectric memories, dynamic random access memories (DRAM), microwave phase shifters, tunable filters, oscillators, sensors, varistors, etc [3,4]. There are several other important ferroelectric materials which were studies such as PZT, BT, ST, BST [4]. Most of the ferroelectric materials have a perovskite structure. The barium titanate BaTiO<sub>3</sub> perovskite structure, it is one of the most widely used ferroelectric materials due to its high dielectric materials and low loss factor that reason has a wide variety of application [5]. SrTiO<sub>3</sub> is usually added as a shifter in order to move the T<sub>c</sub> to lower temperature because it is well established that the Curie temperature of BaSrTiO<sub>3</sub> decreases linearly with a solid solution of Sr<sup>+2</sup> in place of Ba<sup>+2</sup> [6]. Partial substitution of either Ba ions of Ti ions is often employed to modify the nature and temperature of the paraelectric-ferroelectric transition for a particular application [7].

complicated, production costs are increasing enormously and not eco-friendly [9-11]. For these reasons using low-cost, nondoxical and ecologically method is important in order to manufacture CeO<sub>2</sub> nanoparticles [11-13].

In order to improve it electric properties, Sr<sup>+2</sup> ions are introduced into barium titanate to substitute for Ba<sup>+2</sup> ions on A sites and form Ba<sub>1-x</sub>Sr<sub>x</sub>TiO<sub>3</sub> [8]. The perovskite ABX<sub>3</sub> (ABO<sub>3</sub>) structure is given in the different site for (A, B and O) which turn on interplay of competing energies and properties which can be varied significantly with a variation of concentration of Sr<sup>+</sup> ions. B ions are smaller than A ions and turn on make stabilization compound. These oxides appear to have a different structure with a different tolerance factor [9]. Ferroelectric materials with perovskite structure have a large range of application extended from low frequencies to microwave frequencies. For microwave applications require materials have a low dielectric loss. So ferroelectric materials have high dielectric constant and low dielectric loss in low frequencies suitable more for application [10]. BaSrTiO<sub>3</sub> is one of the most ferroelectric materials among the complex oxide perovskite. Barium Strontium Titanate (BST) is a ternary ceramic compound with the stoichiometric formula (Ba<sub>1-x</sub>Sr<sub>x</sub>TiO<sub>3</sub>). For the BaSrTiO<sub>3</sub>, the phase diagram shows an unlimited solution between BaTiO<sub>3</sub> and SrTiO<sub>3</sub> [11]. BST compounds have ferroelectric state and paraelectric state depends on the value of x and Curie temperature. In the ferroelectric state, the BST materials exhibit a high dielectric loss in the microwave range. Therefore for most of the electrically controlled device, the BST materials can be used only in the paraelectric with low frequency [12]. BST exhibits the high dielectric constant as that of BaTiO<sub>3</sub> and the

\*Corresponding author E-mail: [hamed.alwan@alayan.edu.iq](mailto:hamed.alwan@alayan.edu.iq) , [hamedalwan14@gmail.com](mailto:hamedalwan14@gmail.com)

structural stability as that of SrTiO<sub>3</sub> [13]. In recent years, increasing attention has been paid to the synthesis and characterization of nanomaterials because of novel chemical and physical properties arising from the large surface-volume and also the size effect, compared with those counterparts [14]. Ba<sub>1-x</sub>Sr<sub>x</sub>TiO<sub>3</sub> (BST) ferroelectric materials have attracted considerable attentions due to their chemical stability, high permittivity, high tunability and low dielectric losses [15]. The physicochemical properties of these nanomaterials are highly sensitive to their size, shape and composition [16].

The sol-gel method becomes more and more popular for the preparation of high purity BST powders and perovskite oxide powders [17]. The temperature range in which the ferroelectric behaviour is reflected can be easily controlled by adjusting the barium-strontium ratio [18]. Various preparation methods for BST have been investigated, such as hydrothermal, hydrothermal-electrochemical method, solid state reaction spray pyrolysis, chemical co-precipitation methods [19].

In the present study, Ba<sub>1-x</sub>Sr<sub>x</sub>TiO<sub>3</sub> nanopowders were prepared with a different ratio of Sr (0.3, 0.4 and 0.5) by using the sol-gel method, and investigated the influence of these ratios on the microstructure, surface morphology and dielectric properties of all powders.

## 2 Experimental Sections

Synthesis of BST powder was mentioned in a lot of papers. The selected method for BST synthesis depends on some factor such as cost, low temperature, and desired application. The quality of the powders was not only affected by the synthesis route, but also by starting materials used. Ba<sub>1-x</sub>Sr<sub>x</sub>TiO<sub>3</sub> nanopowders with different stoichiometric compositions (x = 0.3, 0.4, 0.5) were synthesized by using sol-gel method. The precursor's materials which were used in this work represent by barium acetate Ba(CH<sub>3</sub>CHOO)<sub>2</sub> (99.5% BDH Chemical-England), strontium acetate Sr(CH<sub>3</sub>CHOO)<sub>2</sub> (Aldrich 99%), and titanium (IV) isopropoxide as a source of barium, strontium, and titanium respectively. Acetic acid CH<sub>3</sub>COOH (Aldrich 97%) was used as the solvent and 2-methoxy ethanol and used also as a stabilizer for Ti (IV) isopropoxide. To obtain the stoichiometric proportions, the appropriate weight of barium acetate and strontium acetate powder was dissolved in a suitable volume of acetic acid. The two solutions separately stirred magnetically at 60°C for 60 min., then mixed together to get (Ba, Sr) solution and refluxed at 110°C for 2 h (till obtained transparent solution which slightly turned to yellow). 2-methoxy ethanol (2-4 ml) was added in Ti (IV) isopropoxide at R.T. (Ba, Sr) solution was added slowly (drop by drop) into Ti (IV) isopropoxide solution, and the pH of the product solution was adjusted in the range of 3 to 5 by adding a buffering agent. Refluxing the mixture again till obtaining a thick white gel. This gel was diluted by distilled water and the solution was mixed by stirring on a hot plate

(60°C) with a magnetic stirrer. All the above steps were repeated for all compositions. Finally, the solutions were dried at 200°C for 2 h to separate the water completely to form amorphous powders with different compositions (Ba<sub>0.7</sub>Sr<sub>0.3</sub>TiO<sub>3</sub>, Ba<sub>0.6</sub>Sr<sub>0.4</sub>TiO<sub>3</sub>, Ba<sub>0.5</sub>Sr<sub>0.5</sub>TiO<sub>3</sub>). The amorphous powders were calcined at 700 C for 2h. The powders were ground in a mortar to obtain a fine powder. The fine powders were pressed by using a hydraulic press as a pelt at pressure equals to 10 tons with 1.2 cm diameter. All pellets sintered at 1000°C for 3 h in the atmosphere. The morphological and composition properties of the sintered pellets were performed by using field emission scanning electron microscopy (FESEM) supplemented with energy dispersive spectroscopy model (Hitachi 4700 field emission microscope). The microstructure of all compounds was recorded at R.T using x-ray powder diffractometer with CuK<sub>α</sub> (λ=1.5418Å<sup>0</sup>, 30 kV, 30 mA) model (Bruker, Germany) in a wide range of 2θ= 20°-80° at scanning rate 1 min<sup>-1</sup>.

## 3 Results and Discussion

Figure (1) shows the EDX spectra of Ba<sub>1-x</sub>Sr<sub>x</sub>TiO<sub>3</sub> with different values of x = 0.3, 0.4, 0.5 which sintered at 1000 °C for 3 h. It is clear that the elements Ba, Sr, Ti, and O were detected in all spectra, and there are no other elements which mean that the pure BST phase was a dominant phase, and no impurities existed. The composition ratios (Ba/Sr) of the as-prepared powders were confirmed using the microarray EDS analysis. Stoichiometric ratios of the Fig. 2 illustrate the FESEM photographs of pure monocrystalline BST ferroelectric samples sintered at 1000 °C for 4 h. As shown in Fig. 2 all samples are dense at the sintering temperature. The particles are a mixture of spherical and nearly cubic in nature and less agglomerated especially for x=0.3 & 0.4. When the Sr<sup>+</sup> content increases to x=0.5 the particle tends to be the spherical shape. The preparation methods possess some parameters to influence more on the size nanostructure of BST. The average grain sizes of the present BST compounds are estimated in the range of 367.23 nm to 63.09 nm when increasing S<sup>+</sup> concentration x=0.3 to x=0.5, respectively. It clear that the particles size of BST decreases with an increment of Sr<sup>+</sup> ions due to the reduction of volume unit cell cause influence the small radius for strontium ion. This result agrees with the results of Azim et. al

main metallic compounds of BST are shown in the table (1) as mass or atomic percentage.

The result values which are given in figure (1) are in acceptable agreement with the stoichiometric ratio for all compounds.

[11], and Yanling et. al [20]. The grain size plays a significant role in determining the electrical properties of the polycrystalline materials. The grain boundaries mainly effect on the conduction mechanism and the relaxation phenomenon of the materials [21].

XRD is the most useful technique to determine the crystal structure, orientation, inter-planar distance, and the crystallite size. The structure of  $Ba_{1-x}Sr_xTiO_3$  powders with different x values which had been produced by the sol-gel method is shown in figure (3). This figure revealed that all samples are polycrystalline in nature.

The XRD pattern of  $Ba_{0.7}Sr_{0.3}TiO_3$  phase has many peaks which related to the tetragonal perovskite and exhibited the P4mm space group with  $a=3.977 \text{ \AA}$ ,  $c=3.9883 \text{ \AA}$ . The c/a ratio is larger than one (the c-axis lattice constant is larger

When  $x=0.4$ , the XRD pattern shows many peaks These peaks are related to the cubic BST phase, and the peaks perfectly match with pdf card no. (00-034-0411), with Pm3m space group and lattice constant  $a=3.965 \text{ \AA}$ .

As seen in Fig.4, the peaks observed for  $Ba_{0.5}Sr_{0.5}TiO_3$  are less intensity than  $x=0.3$  and  $0.4$ , which means that the increasing Sr ratio led to a decrease of the crystallization (as shown in FESEM). This may be due to a small radius of Sr. The data of this sample is in good agreement with the cubic BST phase (PDF card no.00-039-1395).

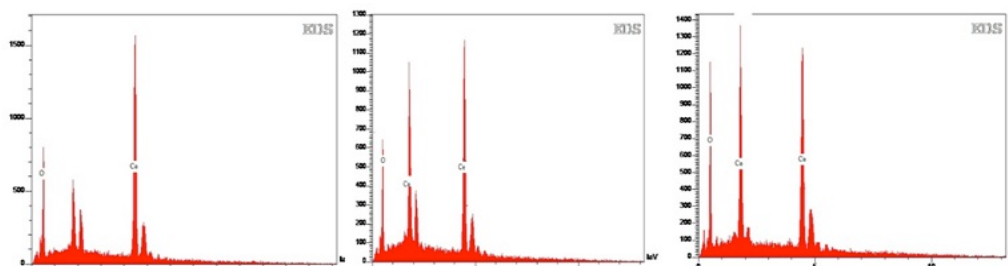


Fig. 1: EDX spectra of CeO2 nano-powders with different sintering temperature.

Table 1: The Calculated and experimental values of the element content in  $Ba_{1-x}Sr_xTiO_3$  compounds.

X	Elements	Line	Theo.values W%	Exp.valuesW%	Theo.Values A%	Exp. Values A%
0.3	O	K <sub>a</sub>	22.14	20.3	60.00	59.32
	Ti	K <sub>a</sub>	22.08	16.29	20.00	15.89
	Sr	L <sub>a</sub>	13.34	16.58	4.60	8.85
	Ba	L <sub>a</sub>	42.44	46.83	15.40	15.94
0.4	O	K <sub>a</sub>	22.50	26.62	60.00	65.19
	Ti	K <sub>a</sub>	22.44	22.58	20.00	18.47
	Sr	L <sub>a</sub>	16.43	11.43	8.00	5.11
	Ba	L <sub>a</sub>	38.63	39.37	12.00	11.32
0.5	O	K <sub>a</sub>	23.04	26.56	60.00	64.65
	Ti	K <sub>a</sub>	22.98	21.6	20.00	17.65
	Sr	L <sub>a</sub>	21.03	19.19	10.00	8.53
	Ba	L <sub>a</sub>	32.96	32.64	10.00	9.26

From XRD analysis, it can be estimated that the tetragonal phase of  $x=0.3$  transforms to cubic phase with increasing Sr ratio to 0.4 and 0.5. Also, the results in Fig(4) clearly show that there are found diffraction peaks from impurity phases even sintering samples at 1000 °C. The peaks appeared at ( $2\theta=24.21, 26.8^\circ$ ), and ( $28.8^\circ$ ) which is belong to intermedia oxycarbonates such  $Ba_2Ti_2O_5CO_3$ ,  $(Ba, Sr)Ti_2O_5CO_3$ , and oxides ( $Sr_2TiO_4$ ,  $SrTiO_4$ ,  $Sr_3Ti_2O_7$ ) at  $44.6^\circ$ [10,21,22].

The major peaks shifted toward higher  $2\theta$  angles when  $Sr^{+}$  ions increased. This shift corresponds to a reduction in unit cell size consistent with the difference between the ionic radii than the a-axis lattice constant). The analysis indicates that the crystalline structure is tetragonal and then indicates that c/a ratio is changing with the composition till reached to a cubic structure.

radii Ba, Sr (1.35, 1.13 Å) which turn on due to a decrease in interatomic space[21,22].

Fig (3) shows the variation of dielectric constant with the frequency. It is observed that with increasing frequency the dielectric constant decreases rapidly and remains constant at higher frequencies. The value of dielectric constant observed at low frequencies is explained on the basis of space charge polarization due to inhomogeneous structure such as porosity, grain structure and impurities. At higher frequencies, dielectric constant remains independent of frequencies due to the inability of dipoles to follow the applied field. So the value of polarization decreasing with increased electric field frequency.

**Table 2:** Structural parameters viz.  $2\theta$  values, inter-planar spacing, Miller indices, and phase of  $Ba_{1-x}Sr_xTiO_3$  powders.

X	$2\theta$ (Deg.)	$d_{hkl}$ Exp.(Å)	$d_{hkl}$ Std.(Å)	hkl	Phase	Card No.
0.3	22.3357	3.9771	3.977	(100)	Tetragonal	00-044-0039
	31.7474	2.8122	2.8162	(101)	Tetragonal	00-044-0039
	39.1636	2.2961	2.2983	(111)	Tetragonal	00-044-0039
	45.5616	1.9885	1.9885	(200)	Tetragonal	00-044-0039
	51.3214	1.7786	1.7795	(201)	Tetragonal	00-044-0039
	56.6061	1.6215	1.6246	(211)	Tetragonal	00-044-0039
	66.3277	1.4060	1.4080	(202)	Tetragonal	00-044-0039
	70.9422	1.2576	1.2610	(212)	Tetragonal	00-044-0039
0.4	22.3984	3.9600	3.9660	(100)	Cubic	00-034-0411
	31.8658	2.8036	2.8060	(110)	Cubic	00-034-0411
	39.3113	2.2891	2.2900	(111)	Cubic	00-034-0411
	45.7322	1.9825	1.9823	(200)	Cubic	00-034-0411
	51.4850	1.7732	1.7735	(210)	Cubic	00-034-0411
	56.8005	1.6195	1.6190	(211)	Cubic	00-034-0411
	66.6377	1.4018	1.4023	(220)	Cubic	00-034-0411
	71.3196	1.2537	1.2530	(221)	Cubic	00-034-0411
0.5	22.4934	3.9470	3.9494	(100)	Cubic	00-039-1395
	32.0312	2.7909	2.7918	(110)	Cubic	00-039-1395
	39.4971	2.2788	2.2796	(111)	Cubic	00-039-1395
	45.9429	1.9735	1.9737	(200)	Cubic	00-039-1395
	51.7535	1.7651	1.7649	(210)	Cubic	00-039-1395
	57.1126	1.6113	1.6113	(211)	Cubic	00-039-1395
	67.0089	1.3954	1.3954	(220)	Cubic	00-039-1395
	71.6718	1.2481	1.2480	(221)	Cubic	00-039-1395

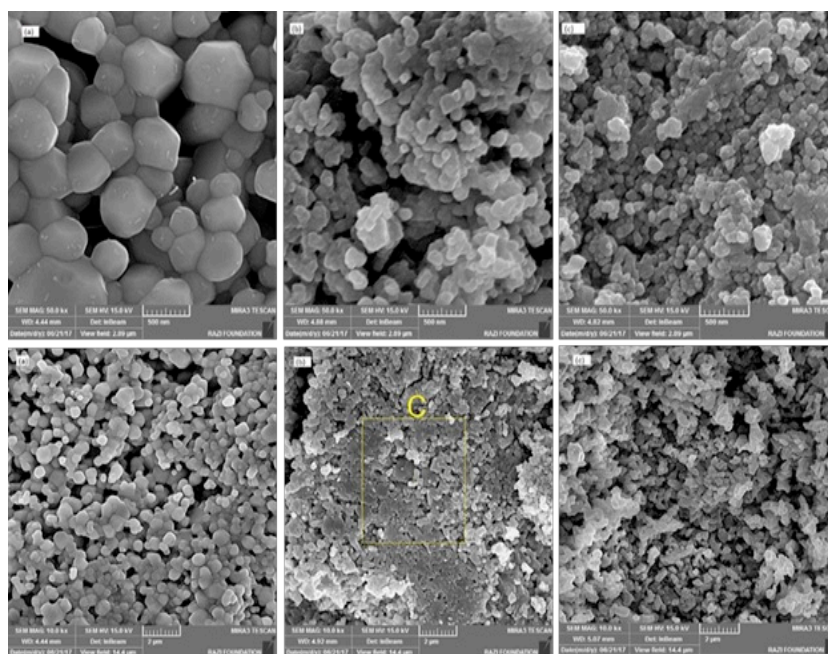


**Fig.2:** Field emission scanning electron microscopy (FESEM) images for  $Ba_{1-x}Sr_xTiO_3$  powders sintered at 1000°C a-  $x=0.3$ , b-  $x=0.4$  and c-  $x=0.5$ .

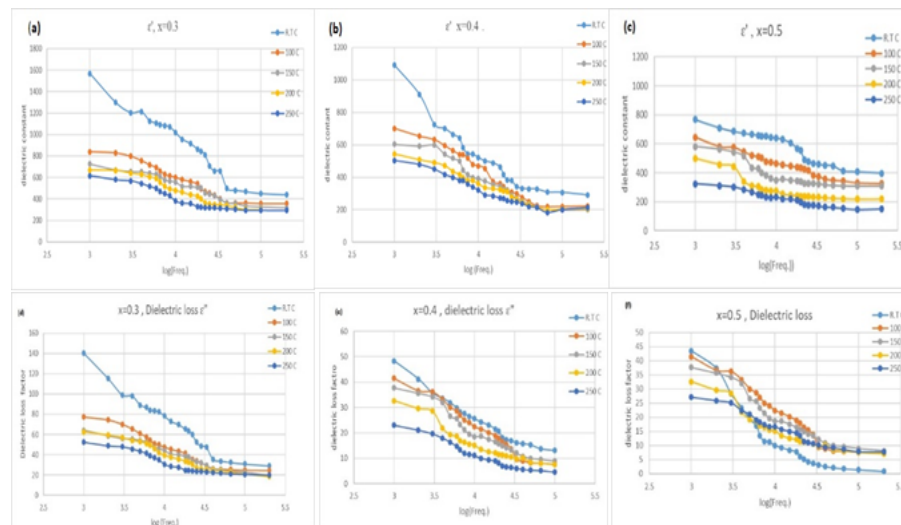


**Fig.3:** shows the variation of dielectric constant with the frequency.

## 4 Conclusions

The BST samples with different stoichiometric composition ( $\text{Ba}_{1-x}\text{Sr}_x\text{TiO}_3$ ) have been successfully synthesized by the sol-gel method. Ceramics materials synthesis from barium acetate, strontium acetate and Titanate isopropoxide with a solvent such as acetic acid and 2-methoxy Ethanol. EDX spectra of as-prepared  $\text{Ba}_{1-x}\text{Sr}_x\text{TiO}_3$  nanoparticles contains Ba, Sr, Ti and O species, and the all experimental ratios of Ba/Sr are close to exact values. FESEM investigation showed that the nanoparticles obtained at 1000 °C the particle size reduction with increasing Sr ratio. The increasing Sr ratio leads to change the phase from tetragonal to cubic when x value change from 0.3 to 0.4, 0.5 and the d-space values decreased with increasing the strontium ions.

Dielectric properties of paraelectric phases  $\text{Ba}_{1-x}\text{Sr}_x\text{TiO}_3$  ceramics with  $x=0.3, 0.4$  and  $0.5$  were investigated in a wide frequency range. Low-frequency measurement in the range 1 KHz to 200 KHz showed a slow decrease of dielectric constant ( $\epsilon'$ ) with the increase in the frequency and increased concentration of strontium ion  $\text{Sr}^{2+}$ . For temperatures between R.T to 250 °C, all the BST samples exhibit same dependence dielectric constant on frequency. At this range, frequency measurements show a decrease of the dielectric constant from around 1500 to 800 at room temperature and for all composites with a different temperature behaviour the same with an increase of x.

**Conflict of interest:** The authors declare no competing financial interest.

## References

- [1] Hamed A. Gatea, The effect of Ba/Sr ratio on the Curie temperature for ferroelectric barium strontium titanate ceramics, *Journal of Advanced Dielectrics.*, **10(5)**, 2020.
- [2] Hamed A. Gatea, The role of substrate temperature on the performance of humidity sensors manufactured from cerium oxide thin films., **31(24)**, 22119-22130, 2020,
- [3] Hang Meng, Shihao Huang, and Yifeng Jiang, The role of oxygen vacancies on resistive switching properties of oxide materials, *AIMS Materials Science.*, **7(5)**, 665–683, 2020.
- [4] T. An, X. Deng, S. Liu, S. Wang, J. Ju, and C. Dou, A Facile Approach for the Synthesis of  $\text{Zn}_2\text{SnO}_4/\text{BiOBr}$  Hybrid Nanocomposites with Improved Visible-Light Photocatalytic Performance, *Ceram. Int.*, **44(8)**, 9742–9745, 2018, doi: 10.1016/j.ceramint.2018.02.206.
- [5] Iqbal S. Naji, and Ameer F. Abulameer , Hamed A. Gatea, Humidity sensing properties of ferroelectric compound  $\text{Ba}_{0.7}\text{Sr}_{0.3}\text{TiO}_3$  thin films grown by pulsed laser deposition, *International Journal of Thin Films Science and Technology.*, **9(2)**, 43, 2020.
- [6] Hamed A. Gatea, Synthesis and characterization of  $\text{BaSrTiO}_3$  perovskite thin films prepared by sol gel technique, *International Journal of Thin Film Science and Technology.*, **10(2)**, 5, 2021.
- [7] G. Balakrishnan et al., Microstructure, optical and dielectric properties of cerium oxide thin films prepared by pulsed laser deposition. *J. Mater. Sci. Mater. Electron.*, **30(17)**, 16548–16553, 2019.
- [8] Hamed A. Gatea, “Impact of sintering temperature on crystallite size and optical properties of  $\text{SnO}_2$

- nanoparticles” *Journal of Physics: Conference Series*, **1829**, 1,2021.
- [9] S. Soni, S. Kumar, B. Dalela, S. Kumar, P. A. Alvi, and S. Dalela, *J. Alloys Compd.*, **752**, 520–531, 2018, doi: 10.1016/j.jallcom.2018.04.157.
- [10] I. Kosacki, T. Suzuki, H. U. Anderson, and P. Colomban, *Solid State Ionics.*, **149(1–2)**, 99–105, 2002, doi: 10.1016/S0167-2738(02)00104-2.
- [11] J. Gong, F. Meng, X. Yang, Z. Fan, and H. Li, *J. Alloys Compd.*, **689**, 606–616, 2016, doi: 10.1016/j.jallcom.2016.08.030.
- [12] E. Swatsitang, S. Phokha, S. Hunpratub, and S. Maensiri, *Phys. B Condens. Matter.*, **485**, 14–20, 2016, doi: 10.1016/j.physb.2016.01.002.
- [13] H. Meng, S. Huang, and Y. Jiang, *AIMS Mater. Sci.*, **7(5)**, 665–683, 2020, doi: 10.3934/matersci.2020.5.665.
- [14] M. Mittal, A. Gupta, and O. P. Pandey, *Sol. Energy*, **165**, March., 206–216, 2018, doi: 10.1016/j.solener.2018.03.033.
- [15] I. T. Liu, M. H. Hon, and L. G. Teoh, *Mater. Trans.*, **58(3)**, 505–508, (2017), doi: 10.2320/matertrans.M2016285.
- [16] Hamed A Gatea “Synthesis and characterization of BaSrTiO<sub>3</sub> perovskite thin films prepared by sol gel technique” *International Journal of Thin Film Science and Technology*, **10**, 2,2021.